Retrieval of ozone and nitrogen dioxide concentrations from Stratospheric Aerosol and Gas Experiment III (SAGE III) measurements using a new algorithm

A. V. Polyakov, Y. M. Timofeyev, D. V. Ionov, and Y. A. Virolainen
Department of Atmospheric Physics, St. Petersburg State University, St. Petersburg, Russia

H. M. Steele[1]
Department of Geography, California State University, Northridge, California, USA

M. J. Newchurch
National Space Science and Technology Center, Atmospheric Science Department, University of Alabama in Huntsville, Huntsville, Alabama, USA

Received 25 May 2004; revised 24 November 2004; accepted 13 January 2005; published 31 March 2005.

[1] We describe a new inversion algorithm developed for the retrieval of atmospheric constituents from Stratospheric Aerosol and Gas Experiment III (SAGE III) solar occultation measurements. The methodology differs from the operational (NASA) algorithm in several important ways. Our algorithm takes account of the finite altitude and spectral resolution of the measurements by integrating over the viewing window spectrally and spatially. We solve the problem nonlinearly by using optimal estimation theory, and we use an aerosol parameterization scheme based on eigenvectors derived from existing empirical and modeled information about their microphysical properties. The first four of these eigenvectors are employed in the retrieval algorithm to describe the spectral variation of the aerosol extinction. We retrieve ozone and nitrogen dioxide number densities and aerosol extinction from transmission measurements at 41 channels from 0.29 to 1.55 μm. In this paper we describe the results of the gas retrievals. Numerical simulations test the accuracy of the scheme, and subsequent retrievals from SAGE III transmission data for the period between May and October 2002 produce profiles of O_3 and NO_2. Comparisons of the O_3 and NO_2 profiles with those obtained using the SAGE III operational algorithm and with those from independent measurements made by satellites, ozonesondes, and lidar indicate agreement in ozone measurements in the middle and upper stratosphere significantly closer than the natural variability and agreement in the lower stratosphere and upper troposphere approximately equal to the natural variability.

Citation: Polyakov, A. V., Y. M. Timofeyev, D. V. Ionov, Y. A. Virolainen, H. M. Steele, and M. J. Newchurch (2005), Retrieval of ozone and nitrogen dioxide concentrations from Stratospheric Aerosol and Gas Experiment III (SAGE III) measurements using a new algorithm, *J. Geophys. Res.*, *110*, D06303, doi:10.1029/2004JD005060.

1. Introduction

[2] In solar occultation experiments, the attenuation of the sun's radiation is recorded by satellite instruments as the satellite orbits the earth and views the sun during each orbital sunrise and sunset. Transmission can be recorded at many wavelengths in the ultraviolet through the infrared. In this work we consider the Stratospheric Aerosol and Gas Experiment III (SAGE III) instrument in particular, in which solar transmission is measured in 87 spectral channels between 290 nm and 1.55 μm [*SAGE III ATBD Team*, 2002b]. Because the satellite views the sun along a slant path through the atmosphere, the problem of retrieving vertical profiles of the atmospheric constituents is twofold. Slant path measurements at different tangent heights (during a sunrise or sunset) can be used together with geometrical considerations to give information on the vertical distribution of constituents, and, with knowledge of the absorption cross section of the atmospheric gases in each spectral channel, the Rayleigh contribution to scattering from the air molecules, and some information regarding the spectral dependence of the aerosol attenuation, spectral information from the array of channels can be used to separate the contributions from

[1] Also at Department of Atmospheric Sciences, University of California, Los Angeles, California, USA.

Copyright 2005 by the American Geophysical Union.
0148-0227/05/2004JD005060$09.00

each constituent. Thus both spatial and spectral inversions must be carried out.

[3] The errors in the retrieval of these atmospheric constituents are the result of a variety of factors including imperfect knowledge of instrument characteristics (e.g., signal noise, aperture shape, and location of measurement channels), imperfect information regarding satellite location and measurement time, errors in the a priori information (e.g., absorption coefficients of different gases), and the inversion method employed (e.g., algorithms for inverting the measured transmission data, and methods for determining the tangent height and accounting for the Sun's "darkening" toward the disk edge). Many of these aspects depend on the particular instrument, and those that can be are quantified as far as possible before launch.

[4] In order to separate the contributions of the various gases and the aerosols from the total attenuation in each channel, some assumption must be made about the optical characteristics of the aerosols. In earlier work, an optimal parameterization scheme for describing the spectral dependence of the aerosol extinction was developed and tested in a series of simulations in which a wide range of stratospheric aerosol conditions was modeled [*Timofeyev et al.*, 2003]. This paper describes the algorithm developed for the retrieval of atmospheric gas concentrations, in particular for NO_2 and ozone. The algorithm is based on work developed for and applied to the Ozone-Mir spectrometer on board the Mir space station [*Poberovskii et al.*, 1999; *Polyakov et al.*, 1999, 2001a].

[5] We describe our application of this scheme to the inversion of transmittance measurements made by the SAGE III spectrometer between May and October 2002 and present vertical profiles of ozone and nitrogen dioxide obtained with our algorithm. These retrievals are compared with those obtained from the operational (NASA) SAGE III algorithm and with independent measurements made by other satellite instruments, ozonesondes and lidar.

2. Retrieval Algorithm

[6] In a solar occultation experiment, the sun's radiance, $J(\lambda_i, h_j)$, at spectral channel i with wavelength λ_i, is recorded as a function of tangent height, h_j and given by

$$J(\lambda_i, h_j) = \int_{h_j-\Delta h_j/2}^{h_j+\Delta h_j/2} \psi(\vartheta(h)) \int_{\lambda_\iota-\Delta\lambda_\iota/2}^{\lambda_\iota+\Delta\lambda_\iota/2} \varphi(\lambda) \mathrm{I}_\oplus(\lambda, \vartheta(h)) \cdot \exp(-\tau(\lambda, h)) d\lambda dh, \quad (1)$$

where φ and ψ are the spectral and angular slit functions of the device, and Δh and $\Delta\lambda$ are the altitude and spectral resolutions of the device. $I_\oplus(\lambda, \vartheta)$ is the intensity of solar radiation at the observation angle, ϑ, and $\tau(\lambda, h)$ is the atmospheric optical depth. The exoatmospheric radiance, $J_0(\lambda_i)$, is then given by

$$J_0(\lambda_i) = \int_{h_j-\Delta h_j/2}^{h_j+\Delta h_j/2} \psi(\vartheta(h)) \int_{\lambda_\iota-\Delta\lambda_\iota/2}^{\lambda_\iota+\Delta\lambda_\iota/2} \varphi(\lambda) \mathrm{I}_\oplus(\lambda, \vartheta(h)) \delta\lambda \delta h. \quad (2)$$

The ratio of these two functions gives the slant path transmittance of the atmosphere. Assuming that the intensity of the solar radiation $I_\oplus(\lambda, \vartheta)$, is constant within the width of each channel, this is given by

$$T(\lambda_i, h_j) = J(\lambda_i, h_j)/J_0(\lambda_i) = \int_{h_j-\Delta h/2}^{h_j+\Delta h/2} \psi(\vartheta(h)) \int_{\lambda_\iota-\Delta\lambda_\iota/2}^{\lambda_\iota+\Delta\lambda_\iota/2} \varphi(\lambda) \exp(-\tau(\lambda, h)) \delta\lambda \delta h. \quad (3)$$

The atmospheric optical depth, τ, is given by

$$\tau(\lambda, h) = \int_S k(\lambda, z(s)) ds = \int_S k_{o_3} N^{O_3} ds + \int_S k_{NO_2} N^{NO_2} ds + \int_S \alpha_{Rayleigh} ds + \int_S \alpha_{aerosol} ds, \quad (4)$$

where S is the slant path through the atmosphere at tangent height h, ds is an element of this path, $z(s)$ is the altitude of the slant path, and $k(\lambda, z)$ is the total coefficient of extinction and attenuation due to all gases and aerosols and comprises the O_3 and NO_2 absorption coefficients, k_{o_3} and k_{NO_2}, and Rayleigh and aerosol extinction coefficients, $\alpha_{Rayleigh}$ and $\alpha_{aerosol}$. Equations (3) and (4) are the basis for formulating and solving the nonlinear inverse problem with respect to retrieving vertical profiles of ozone concentration, $N^{O_3}(z)$, nitrogen dioxide, $N^{NO_2}(z)$, and aerosol extinction, $\alpha_{aerosol}(z)$. This method is slow because of the necessity of carrying out both spectral and angular integration, and differs from the method used for routine processing of the SAGE III measurements [*SAGE III ATBD Team*, 2002b] in which it is assumed that the atmospheric transmittance function can be approximated by the exponential dependence from the atmospheric optical depth $\bar{\tau}(\lambda_i, h_j)$ averaged over discrete spectral intervals λ_i,

$$T(\lambda_i, h_j) \approx \exp(-\bar{\tau}(\lambda_i, h_j)), \quad (5)$$

so that

$$\bar{\tau}(\lambda_i, h_j) = -\ln(T(\lambda_i, h_j)) = \int_S \bar{k}(\lambda_i, z(s)) ds, \quad (6)$$

where $\bar{k}(\lambda_i, z)$ is the mean effective absorption coefficient for the spectral interval under consideration at the relevant tangent height. Another difference between our inversion algorithm (referred to as the SPbSU algorithm) and the SAGE III operational (NASA) algorithm is in the treatment of aerosols. In our method, the aerosol extinction coefficient is approximated by a linear expansion in terms of basis functions which were derived from numerical modeling using a large database of aerosol size and composition. These basis functions are optimal in the sense that the fewest number of terms are required to model the greatest part of the expected variability in the measured

aerosols [*Polyakov et al.*, 2001b; *Timofeyev et al.*, 2003; *Virolainen et al.*, 2004] The aerosol extinction coefficient, $\alpha_{aerosol}(\lambda, z)$, is thence approximated by the expansion,

$$\alpha_{aerosol}(\lambda, z) = \bar{\alpha}_{aerosol}(\lambda) + \sum_{k=1,4} a_k(z) W_k(\lambda), \quad (7)$$

where $\bar{\alpha}_{aerosol}(\lambda)$ is the mean function of the spectral dependence of aerosol extinction averaged over all altitudes, and $W_k(\lambda)$, $k = 1, 4$ are the first four eigenvectors of the spectral covariance matrix. Statistical aerosol models were used to define these. These models are based on a large database that includes volcanic and background aerosols, and aerosols of many different sizes and compositions. For a full description see *Timofeyev et al.* [2003]. Thus four parameters, $a_k(z)$, must be retrieved to describe aerosol extinction at each altitude.

[7] The Rayleigh contribution to the extinction is calculated using well-known formulae on the basis of the temperature and pressure profiles given in the SAGE III level 1b data [*SAGE III ATBD Team*, 2002a]. The temperature-dependent contributions to the total optical depth from ozone and NO_2 are derived from the O_3 and NO_2 absorption cross sections given by *Bass and Paur* [1984], *Burkholder and Talukdar* [1994], and *Schneider et al.* [1987].

[8] In order to solve the set of equations we discretize the continuous altitude functions to a finite dimensional representation using the SAGE III altitude grid (0–100 km with a 0.5 km step) and combine all ($p = 6$) parameters to be determined in a vector **x**. This vector thus comprises the gas number density vectors, N^{O_3} and N^{NO_2}, giving gas concentration at each altitude, and the four aerosol expansion coefficients, $a_k(z)$, at each altitude,

$$(x_1, x_2, \ldots, x_{1200}) = \left(N_1^{O_3}, \ldots, N_{200}^{O_3}, N_1^{NO_2}, \ldots, N_{200}^{NO_2}, a_1^1, \ldots, a_{200}^1, a_1^2, \ldots, a_{200}^2, \ldots, \ldots, a_1^4, \ldots, a_{200}^4\right).$$

Subscripts refer to the 200 altitude grid points between 0 and 100 km.

[9] We solve the retrieval problem through optimal estimation [*Rodgers*, 2000]. For this nonlinear problem the nth iteration of the solution vector $\hat{x}_n$ is obtained by iterating from the a priori vector x_a according to *Rodgers* [2000], *Polyakov* [1996], and *Lumpe et al.* [1997],

$$\hat{x}_{n+1} = x_a + \left(S_a^{-1} + K_n^T S_y^{-1} K_n\right)^{-1} K_n^T S_y^{-1} [y - y_n + K_n(\hat{x}_n - x_a)], \quad (8)$$

where y = [$T(\lambda_1, h_1)$, $T(\lambda_2, h_1)$,. . .., $T(\lambda_m, h_1)$, $T(\lambda_1, h_2)$,. . .., $T(\lambda_m, h_2)$, $T(\lambda_1, h_l)$,. . .., $T(\lambda_m, h_l)$] is the vector of transmission measurements at m wavelengths and l altitude values. These transmission data have associated with them an (ml x ml) covariance matrix S_y, with diagonal elements set to be the assumed error variances at each wavelength-altitude combination. Off-diagonal elements of S_y are assumed to be zero.

[10] The a priori vector x_a was derived from climatological mean profiles [*Anderson et al.*, 1986]. In the case of O_3 a midlatitude summer profile was used, and for NO_2, the global mean profile. S_a is the (1200 × 1200) a priori covariance matrix, used to constrain the retrieval. Cross correlations between components (O_3, NO_2 and aerosol) are assumed to be absent. The a priori covariance matrix, S_a, was thus constructed from three diagonal square cells—one for each of O_3, NO_2 and aerosol. For the gases the elements of S_a are given by

$$S(h_i, h_j) = \sigma(h_i)\bar{N}(h_i)\sigma(h_j)\bar{N}(h_j) \exp\left(-\frac{|h_i - h_j|}{r}\right), \quad (9)$$

where $\bar{N}(h)$ is the mean profile of the gas number density and $\sigma(h)$ is its standard deviation (set to be 0.6 $\bar{N}(h)$ for O_3 and 1.0 $\bar{N}(h)$ for NO_2). r is the correlation radius, which we set to 5 km. A priori information for the aerosols (mean profiles and the covariance matrix of $a_k(z)$) and the quasi-empirical orthogonal basis set, $W_k(\lambda)$, were determined by numerical simulation of the aerosol variability [*Polyakov et al.*, 2001a; *Timofeyev et al.*, 2003; *Virolainen et al.*, 2004]. The (ml × pl) kernel (or Jacobian) matrix K_n is the derivative of the transmission with respect to the (pl) retrieval parameters, x:

$$K_n = \left.\frac{\partial T}{\partial x}\right|_{x=x_n}. \quad (10)$$

These elements are derived from the forward model (3) which relates the transmission, T, to the gas concentrations through (4). K_n was calculated numerically at each iteration using exact analytical expressions. Iteration is allowed to proceed until a convergence criterion is met based upon the smallness of the difference $x_{k+1} - x_k$. According to theory (assuming normally distributed random errors) the uncertainty in the retrieval parameters is then given by the covariance matrix of the solution errors, $\hat{S}$:

$$\hat{S} = \left(S_a^{-1} + K^T S_y^{-1} K\right)^{-1}. \quad (11)$$

[11] In reality convergence is difficult to achieve as the steps tend to oscillate around the solution. Thus an extra term was added to the function to be minimized on the basis of the difference, $x_{k+1} - x_k$, to help in reaching convergence. The details of this are described in Appendix A. The retrieval of vertical profiles of ozone, nitrogen dioxide, and aerosol extinction was carried out as described above using 41 channels of the SAGE III measurements. We omitted the 290 nm and 384 nm channels, which we believe may overestimate transmittance below 55 km and below 30 km respectively, and also omit from consideration the oxygen and water vapor bands at 758–770 nm and 933–960 nm.

[12] One of the important characteristics of remote sensing measurements is the vertical resolution of the retrieved atmospheric constituents. This vertical resolution is determined not so much by the altitude grid applied in the retrieval as by the peculiarities of radiation transfer through the atmosphere in the region of interest—in our case, by the spatial distribution in altitude of the attenuating atmospheric layers. The algorithm for solving the inverse problem also influences to some degree the vertical resolution of the retrievals. To determine the vertical resolution in our case, we calculated the widths of the averaging kernels [see, e.g., *Rodgers*, 2000] for the inverse operator of our retrieval algorithm. These values were close to 1.5 km, even though we use an altitude step of 0.5 km in the retrievals. Thus

Table 1. Errors Associated With Retrieving the Atmospheric Constituents and the Chi-Square Statistic in the Fits

		Retrieval Errors				
Model Number	Atmospheric Model	Aerosol Extinction Coefficient,[a] km^{-1}	Ozone (12–40 km), Relative Error, %	Ozone (40–70 km), Relative Error, %	NO_2 (20–45 km), Relative Error, %	Chi-Square Statistic[b]
0	Base model	0.64E-4	5.4	4.9	6.0	0.96
1	NO_2*2,	0.65E-4	5.4	4.9	3.4	0.96
2	NO_2*2, noise[c]	0.65E-4	5.4	4.9	3.4	0.96
3	Aerosol 42[d]	0.14E-3	12	5.4	8.6	0.98
4	Aerosol 48[d]	0.69E-4	5.6	5.0	8.3	0.97
5	Aerosol 48,[d] three vectors	0.66E-4	5.6	6.1	7.8	1.07
6	Aerosol 48,[d] two vectors	0.13E-3	9.1	15	60	9.0
7	Measurement error*2	0.84E-4	7.4	5.9	6.8	0.97
8	Measurement error/2	0.44–4	3.9	4.0	5.0	0.96
9	H[e] 0.5	0.18–3	9.6	12.4	16.8	1.01

[a]Read 0.64E-4 as 0.64×10^{-4}.
[b]Chi-square statistic is given by $\sqrt{\frac{1}{ml}\sum_{i,j}\left(\frac{T_{meas}(\lambda_i,h_j)-T_{calc}(\lambda_i,h_j)}{\sigma_{i,j}}\right)^2}$. (See text.)
[c]This is a different noise assignment (covariance matrix S_y) than the standard one used.
[d]These are model numbers taken from *Polyakov et al.* [2001b]. Model 42 corresponds to a heavy aerosol loading and model 48 to background aerosol.
[e]All heights have been increased by 0.5 km.

laminated structures with a width of less than about 1.5 km, which might occur in the gas profiles, will not be seen in our retrieved profiles since such fine structured oscillations will be smoothed out with a sliding average over a width of about 1.5 km.

3. Numerical Simulations

[13] In order to study the potential errors associated with using our algorithm to retrieve the gaseous and aerosol composition of the atmosphere from SAGE III transmission data [*SAGE III ATBD Team*, 2002a], we carried out a number of closed-loop numerical simulations as described in detail by *Polyakov and Timofeyev* [2003a, 2003b]. A base model of the atmosphere was generated from three different mean climatic ozone profiles, one for each of the tropics, the middle latitude winter, and the subarctic winter. A mean global profile was used for NO_2, and a background aerosol extinction profile was generated from an ensemble of aerosol size distributions [*Polyakov et al.*, 2001b; *Timofeyev et al.*, 2003]. Typical profiles of temperature and pressure were taken from SAGE III data. Atmospheric transmittance functions for this base model at the SAGE III measurement channels were then generated using our forward model, and measurement error estimates from a typical SAGE III event added to these using a random number generator. These transmittance functions were then used as input to the inverse problem and the retrieved O_3, NO_2 and aerosol extinction profiles compared with the exact (known) values to estimate retrieval errors. This cycle of calculating the forward model and performing the inverse task was repeated with a variety of atmospheric conditions to evaluate the performance of our scheme and the propagation of experimental error into the results.

[14] Table 1 lists the different atmospheric conditions used in the numerical experiments and the corresponding retrieval errors. The last column of the table gives the chi-square statistic which measure the goodness of the fit, and is given by $\sqrt{\frac{1}{ml}\sum_{i,j}\left(\frac{T_{meas}(\lambda_i,h_j)-T_{calc}(\lambda_i,h_j)}{\sigma_{i,j}}\right)^2}$, where T_{meas} and T_{calc} are the measured and modeled transmittances, and σ_{ij} are the estimated errors in the measured transmittances. For retrievals which meet the error criteria exactly, the chi-square statistic has the value 1.

[15] Row 0 corresponds to the base model described above. For this case, the O_3 retrieval errors are approximately 5% throughout the stratosphere and mesosphere, and for NO_2 the errors are 6% between 20 and 45 km. The next simulation shows the result of doubling the NO_2 content. This change leads to a decrease in the NO_2 relative retrieval error from 6 to 3.4% and no change in the O_3 retrieval error. Subsequent rows show the influence of varying the noise realization from the standard used in the base model, changing the aerosol loading and parameterization, and introducing an error in the altitude. Row 2 shows the influence of a different noise assignment to the measurements; row 3 uses a more turbid atmosphere—which affects not only the aerosol extinction error but also increases gas retrieval errors to 12% for stratospheric ozone and 8.6% for NO_2 as a result of the decrease in atmospheric transmittance. Row 4 shows the case of a different background aerosol, and produces similar errors to the base model. Rows 5 and 6 show the effect on the retrieval errors, of reducing the number of independent parameters describing the aerosol extinction (the number of terms in equation (7)). In row 5, the solution of the inverse problem is performed using only three rather than four parameters, in row 6 this is further reduced to just two parameters. It is seen that decreasing the number of parameters to three has little effect on the retrieval errors, but the tightening of the constraint increases the systematic errors (or relative residual). The fit is still relatively good with three parameters, but with only two parameters, the fit is much worse. Retrieval errors have increased for all the constituents, and in addition, the normalized residual in the fit is very large, some nine times larger than the other cases presented here. These analyses testify to the inadequacy of a two-parameter model in describing aerosol extinction. In rows 7 and 8, the influence of measurement accuracy on retrieval errors is analyzed. Transmittance errors at all wavelengths were increased (in row 7) and decreased (in row 8) by a factor of two relative to those of the base model (which were taken from a sample SAGE III measurement and are applied in all cases unless otherwise specified). Such error changes affect the retrieval errors in the atmospheric con-

Table 2. Independent Measurements by Month and Latitude Zone

	Number of Measurements			
	Sondes	Lidars	HALOE	HALOE Local Sunset
Latitude Zone				
42.94N–53.30N	40	14	0	0
65.55N–79.47N	4	6	87	0
46.83S–54.54S	8	3	60	43
Month				
May	10	3	0	0
June	13	3	0	0
July	17	7	0	0
Aug.	4	1	35	31
Sept.	0	5	99	12
Oct.	8	4	13	0

stituents, but not unreasonably. In the last row, the influence of an error introduced into the measurement referencing height is tested by increasing all tangent heights by 0.5 km. Such an error leads to a dramatic and potentially serious increase in the errors associated with solving the inverse problem.

4. SAGE III Retrievals

[16] In this section we describe retrievals of O_3 and NO_2 from SAGE III measurements made between May and October 2002. In the mesosphere, our ozone retrievals are compared with measurements made by the CRISTA [*Kostsov et al.*, 2004] and HALOE [*Bruhl et al.*, 1996] (data from http://haloedata.larc.nasa.gov/) satellite instruments, climatological model profiles, and SAGE III ozone retrievals obtained via NASA's operational algorithm. In the stratosphere, we compare our retrievals with those of the SAGE III operational algorithm and with independent measurements made by ozonesondes, lidar, and HALOE. SAGE III retrievals yield number density, so this unit is employed in comparisons with independent measurements wherever these also employ number density. Where comparison data are available only in mixing ratio, the SAGE III data are converted using the meteorological data supplied for each occultation.

[17] For the period between May and October 2002, for which we obtained the SAGE III transmission data, we located independent measurements within 550 km and 24 hours. This search yielded some 52 O_3 profiles from 11 ozonesonde stations (*WMO World Data Center for Ozone and Ultraviolet Radiation*, ftp://ftp.tor.ec.gc.ca), 23 O_3 profiles from 5 lidar stations (http://nadir.nilu.no) and 147 HALOE O_3 and NO_2 profiles [*Bruhl et al.*, 1996]. Because the SAGE III inversion algorithms do not account for spatial inhomogeneity resulting from diurnal changes, we restricted our comparisons with HALOE data to local sunset only cases. This significantly reduced the number of coincidences from 147 to 43. In addition, CRISTA measurements [*Kostsov et al.*, 2004] were obtained for validation of mesospheric ozone. These independent measurements are listed in Table 2.

4.1. Ozone Retrievals

[18] In the SAGE III spectral range, ozone absorbs in two diapasons—in the shortwave range between 290 and 330 nm and in the visible, with a maximum at 600 nm. The UV absorption band can be used to obtain ozone concentrations at tangent heights of 100–40 km. Below this, the atmosphere becomes opaque as a result of molecular scattering and ozone absorption. The Chappuis band (600 nm) is weaker and can be used below 50–60 km. As distinct from the SAGE III operational algorithm, in which the shortwave range is used for altitudes above 50 km, and the longwave range, for altitudes below 50 km, in our algorithm all wavelengths are considered simultaneously—with the exception of the 290 nm channel which is included only at altitudes above 55 km.

[19] Figure 1 shows examples of the ozone profiles retrieved from the SAGE III data using our inversion scheme and demonstrates the spatial-temporal variability of O_3 profiles from 54°S to 79°N between May and October. Fine structure is seen in the profiles, as is a secondary maximum in the polar profile, and the mesospheric minimum at 70–80 km.

[20] In Figure 2 we show a comparison of the mean retrieved profile obtained from 16 SAGE III events taken in July 2002 between 43°N and 47°N using the SPbSU algorithm, with July models at latitudes of 40°N and 50°N [*Keating et al.*, 1989]. The models give very close agreement with our retrievals.

[21] In the mesosphere, we used CRISTA profiles derived from infrared limb spectra between 4 and 12 November 1994 for comparison with our retrievals. The CRISTA O_3 profiles at 50–100 km were derived using a special algorithm which does not assume local thermodynamic equilibrium [*Kostsov et al.*, 2004]. Because of the large temporal differences in the measurements we can compare only mean profiles and their variances. To make the geometrical configuration as close as possible, we used only those CRISTA measurements taken during sunrises and sunsets at zenith angles of 80°–100°. These measurements were made at latitudes of 41°N–63°N and 16°S–53°S. The mean

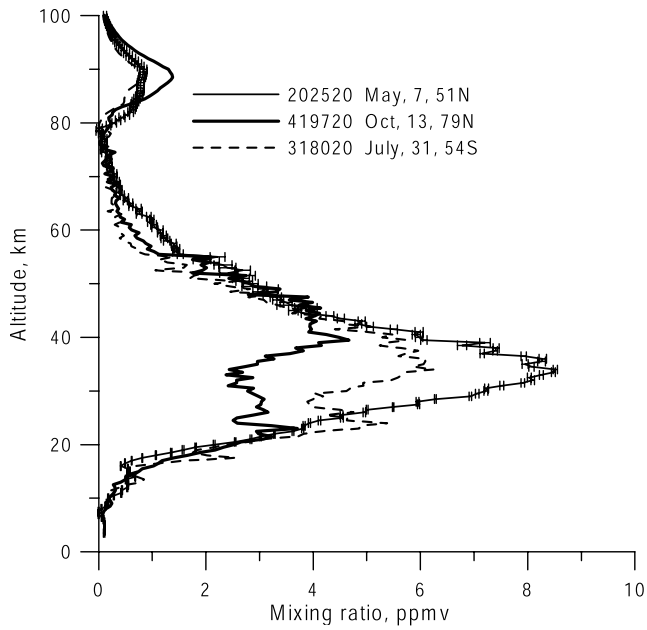

Figure 1. Some example ozone profiles retrieved from SAGE III transmission data using the SPbSU algorithm.

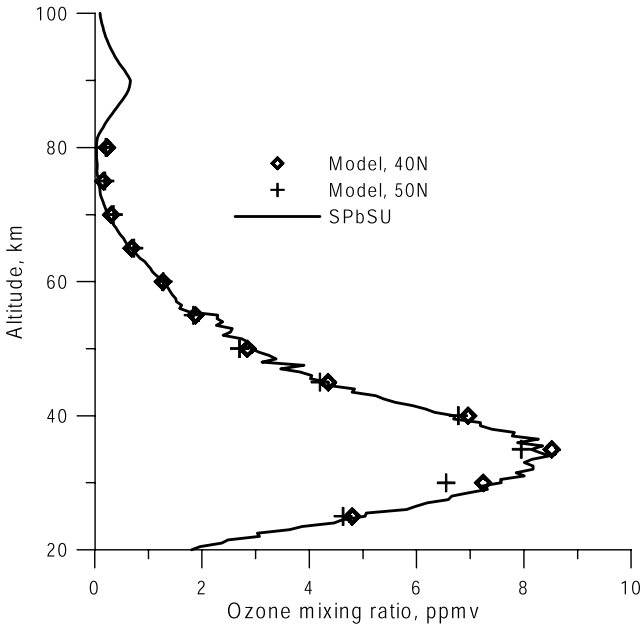

Figure 2. Comparison of mean model profiles for July at 40°N and 50°N with the mean SPbSU profile for July for 16 events between 43°N and 47°N.

of these profiles was compared with SAGE III data for the May–October 2002 time period at latitudes of 43°N–69°N, 47°S–54°S. In Figure 3 we show the comparison. Both profiles show a minimum in the ozone number density at 80 km, and coincide very closely at 55–65 km. At all altitudes, the mean profiles overlap within the standard deviation of the data but there are some differences between them. Above 65 km, SAGE III gives lower values of O_3 number density. Below 65 km, the opposite holds. There is also a small difference in the altitude of the O_3 minimum at 80–85 km. Bearing in mind the natural O_3 variability and the large temporal measurement difference (8 years), the measurements are in reasonable agreement.

[22] HALOE mesospheric ozone measurements were also compared with SAGE III. As mentioned above, 147 HALOE profiles collocated in time and space with SAGE III data were obtained. However, this comparison includes both sunrise and sunset occultations. Because the SAGE III algorithms assume horizontal homogeneity and do not account for the inhomogeneity introduced by diurnal variations, we chose to compare only those local sunset observations, which reduces the number of comparisons to 43. Figure 4 shows a comparison of the mean of these profiles with the mean O_3 profiles retrieved from SAGE III measurements by the two algorithms, SPbSU and the operational (NASA) algorithm (SAGE III level 2 data). The horizontal lines show the standard deviation in the HALOE data. These data agree well in the lower mesosphere where RMS differences between the SAGE III algorithms and HALOE are less than 20%. Above 65 km, the differences increase, reaching as much as 100% in the middle mesosphere, but then dropping off slightly at higher altitudes. At 70–80 km there is a minimum in the ozone and although the difference in the means of the three profiles is quite small (Figure 4 (left)), the relative RMS deviation between SPbSU and HALOE shown in Figure 4 (right) reaches a maximum value of over 100% here. This discrepancy indicates significant differences between individual profiles at this altitude. However, the smallness of the absolute value serves to increase the relative error significantly. At 80–90 km the RMS relative differences decrease to around 40–80% as a result of the increase in the absolute value of the ozone mixing ratio. Comparing SPbSU retrievals with the SAGE III algorithm, differences are small below 65 km, but increase significantly in the upper mesosphere above 75 km. The SPbSU algorithm gives better agreement with HALOE than the SAGE III operational algorithm at these high altitudes. Differences arise for a variety of reasons, but most notably because retrieval errors increase with altitude. Also, diurnal effects which are treated in the HALOE algorithm, but not in the SAGE III algorithms are more important at higher altitudes.

[23] There are more opportunities for comparisons of SAGE III ozone data in the stratosphere. In addition to satellites, there are networks of ozonesonde and lidar stations. These stations are part of the World Ozone and Ultraviolet Radiation Data Center (WOUDC) and the data are accessible online (http://www.msc-smc.ec.gc.ca/woudc). Fifty-two ozonesonde profiles were chosen for validation of our SAGE III retrievals. These measurements provide ozone partial pressure and the corresponding air pressure and temperature profiles, which allow for conversion to ozone number density. An example comparison of a single SAGE III profile with an ozonesonde measurement is given in Figure 5. The fine structure in the ozone profile (in particular, a secondary maximum at 13–14 km, and a step near 21–23 km) is well resolved. At altitudes above 16 km the difference in the profiles is less than 10%, but increases significantly below this altitude because of the smaller ozone concentration in the lowest part of the stratosphere.

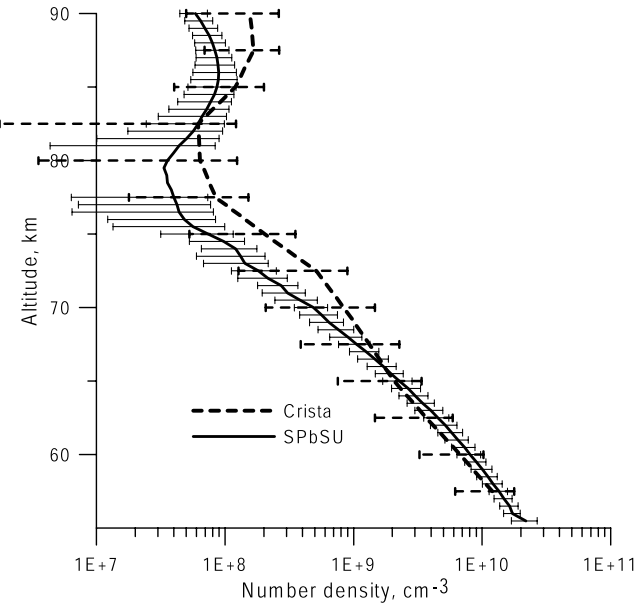

Figure 3. Comparison of mean profiles of ozone number density retrieved from CRISTA and SAGE III data. Horizontal segments show the standard deviation in the measurements.

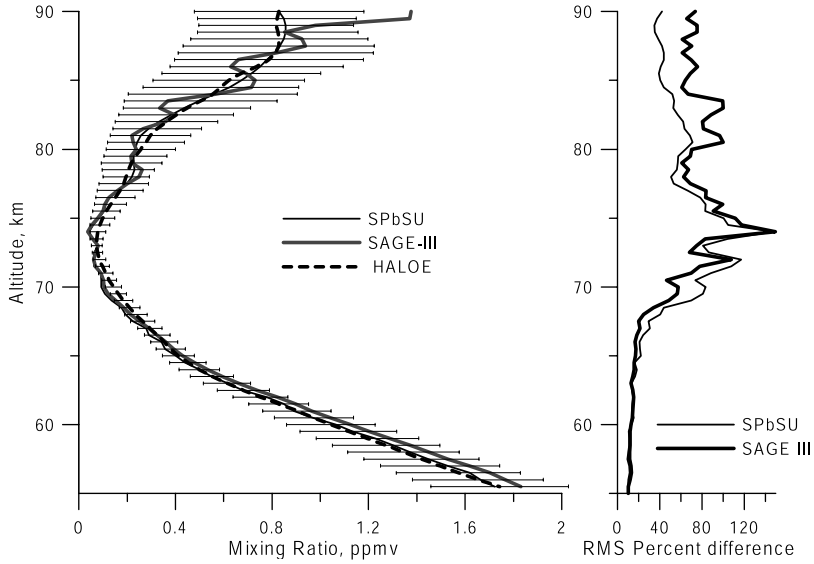

Figure 4. (left) Comparison of ozone mean mixing ratio profiles from local sunset-coincident measurements of HALOE and SAGE III (operational and SPbSU algorithms). Horizontal segments show the standard deviation of HALOE profiles. (right) RMS difference between the SAGE III and HALOE profiles.

[24] In Figure 6 we show a comparison between a lidar profile from Hohenpeissenberg and retrievals performed by the SPbSU and operational (NASA) algorithms from SAGE III data. The lidar and SAGE data locations are only 18 km and 1 hour apart. The two satellite retrievals agree closely in magnitude and in fine structure and differ by ±10% from the lidar for most of the stratosphere. The largest difference with the lidar profile, of 30%, occurs at an altitude of 17 km. Because of the similarity in the two SAGE III retrievals this suggests some real differences between the ozone profiles measured by the two instruments. It is possible that the averaging of the SAGE III data over the slant path through the atmosphere and horizontal ozone variations produce some differences between the ozone measurements.

[25] In Figure 7, we show the statistical summary of our comparisons between all the ozonesonde profiles, and the SAGE III data retrieved via the SPbSU and operational algorithms. The natural variability of the ozonesonde measurements (standard deviation in profiles), together with the

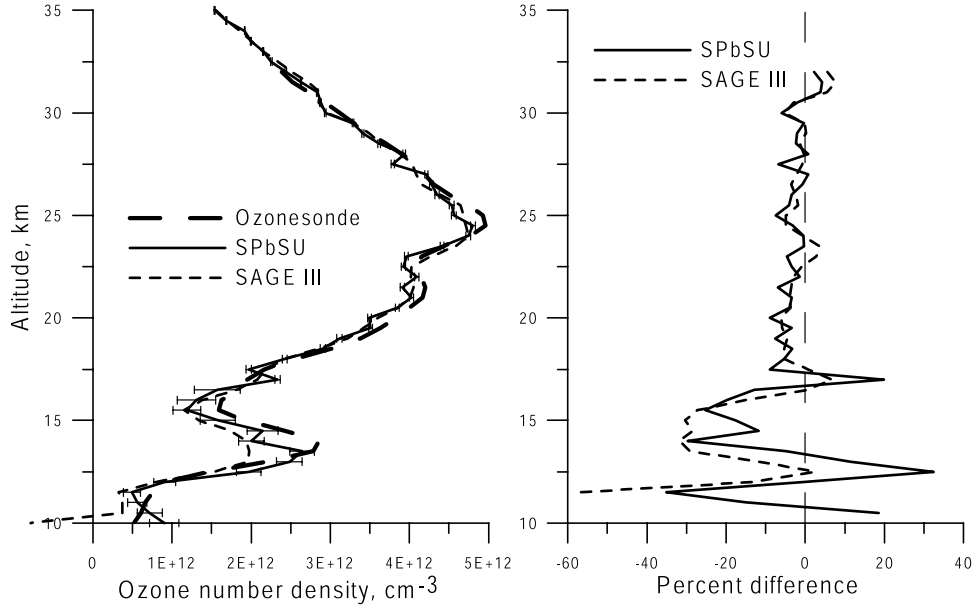

Figure 5. Comparison of an ozonesonde profile from Payerne and the SPbSU and the operational algorithms profile retrieved from the closest SAGE III event (ID 302420, taken on 19 July 2002 at 1911, location 44.56°N, 5.87°E). The distance between measurements is 220 km, and the time difference is 8 hours.

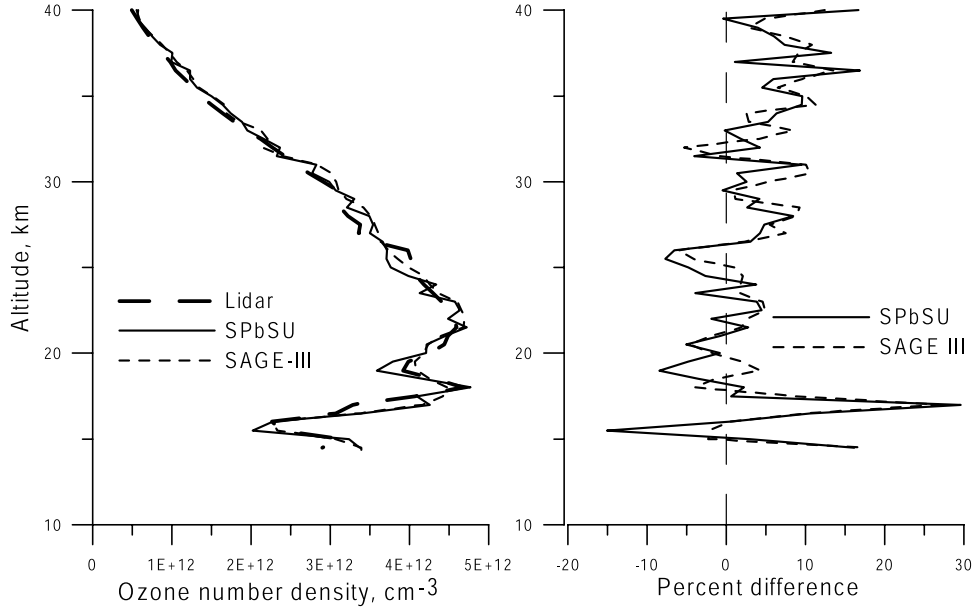

Figure 6. Comparison of a SAGE III ozone profile (ID 221720, on 21 May 2002 at 1849, location 47.69°N, 10.83°E) from the SPbSU and the operational algorithms with a lidar profile from Hohenpeissenberg. Profiles were measured 18 km and 1 hour apart.

mean and RMS differences between the SAGE III data and these measurements are shown. Because of the differences in time and space between sets of measurements, differences between the ozone profiles have at least two sources—natural spatial-temporal variability within the limits of our collocation criteria, and the difference between the observation methods. The relative importance of these two factors changes with altitude.

[26] At 10–35 km, there is an overestimate of the ozone number density by the SAGE III retrieved profiles in

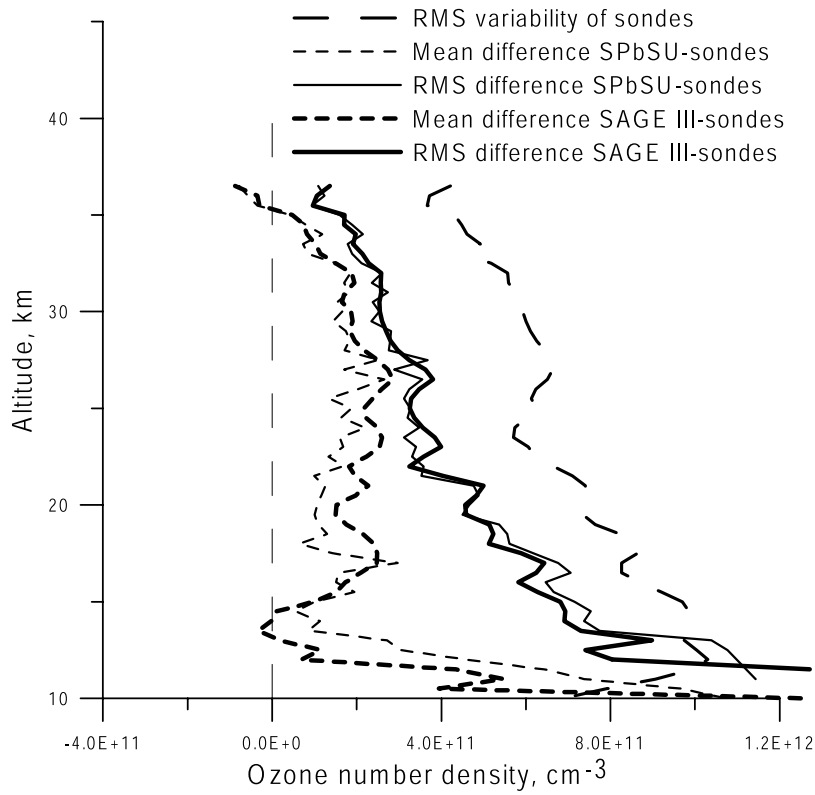

Figure 7. Statistics of the differences between the SAGE III ozone profiles retrieved by the SPbSU algorithm and ozonesonde data.

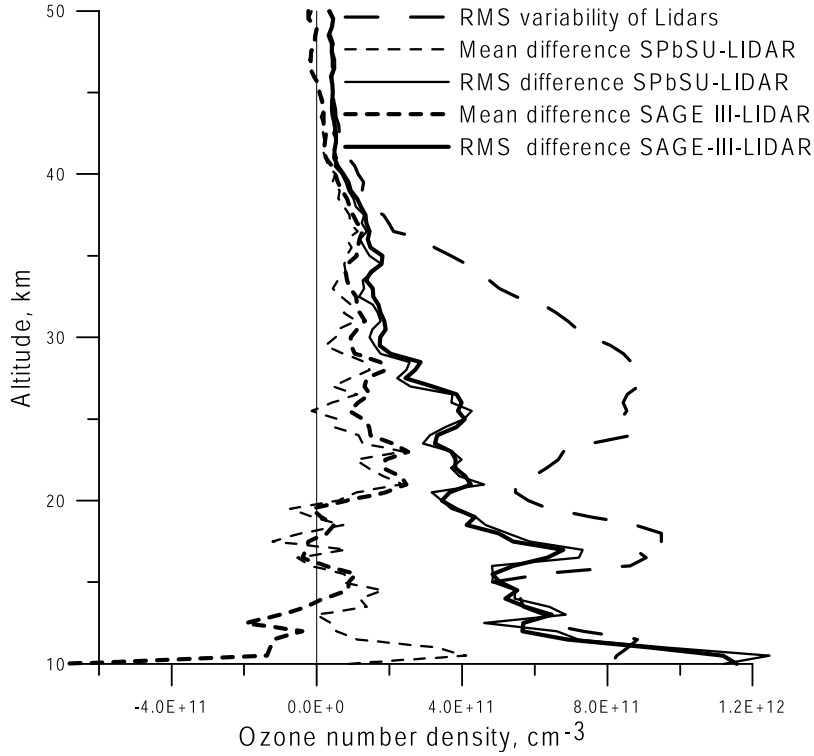

Figure 8. Statistics of the differences between the SAGE III ozone profiles retrieved by the SPbSU algorithm, the SAGE III operational algorithm, and the lidar measurements.

comparison with the ozonesonde data. There is little difference between the random component (RMS) of the difference at 25–35 km and the mean difference, which suggests that most of the difference arises from a real systematic difference between the profiles in this altitude region. In the 15–35 km altitude range, the natural profile variability is significantly greater than the RMS difference between the retrieved and measured profiles. Thus the SAGE III satellite measurements provide new information on the ozone content at these altitudes. Below 15 km, the RMS difference increases and approaches the natural variability of the ozonesonde measurements, so SAGE III contributes comparable accuracy at these low altitudes. The retrievals obtained via the two different SAGE III algorithms show very similar statistics in comparison to the ozonesonde data.

[27] Ozone number density profiles obtained from 23 lidar soundings are compared with collocated SAGE III events in Figure 8. Presented here are the statistics of this set of comparisons showing the mean and RMS differences between the lidar data and those obtained for the SPbSU algorithm and the operational algorithm applied to the same SAGE III data. Also shown is the standard deviation (RMS variability) of the lidar data. At 20–40 km, there is a systematic overestimation of ozone values by both algorithms using SAGE III data in comparison with lidar data, but the overestimate is only about half of what it was for ozonesondes. No systematic difference exists between the satellite and lidar profiles at 15–20 km but below 15 km the satellite data again exceed the lidar data. In general, the patterns of mean and RMS difference are very similar for the two SAGE III retrieval algorithms, but below 15 km the biases in the two algorithms are opposite from each other. The altitude dependence of the RMS differences is similar for lidar and the ozonesondes above 15 km and these differences are smaller than the natural variability of the data. At 20–35 km the RMS differences are a factor of 2–3 smaller than the standard deviation of the data.

[28] It is instructive to see how well the ozonesonde and lidar data agree with each other. When data from seven collocated ozonesonde and lidar measurements were compared (Figure 9), no systematic differences were found between them between 20 and 33 km. In this altitude range, the RMS difference between profiles was also small—less than 10%. However, below 15 km both systematic and RMS differences became much larger, increasing to 60 and 80% respectively at 12 km. This level of agreement suggests that a real part of differences seen between measurements at these altitudes in the lowest part of the stratosphere is a result of natural (spatial and temporal) ozone variability at these altitudes, and does not occur only in satellite experiments as a result of the problem of separating aerosol and ozone contributions to extinction. Satellite measurements give average values over a horizontal path of 200–400 km depending on the measurement altitude. Ozonesonde measurements are made in situ with a vertical resolution of approximately 100 m and can deviate from their launch location by 100–200 km. Lidar measurements are normally performed looking vertically upward and thus have very high spatial resolution in the horizontal. If the ozone field is horizontally homogeneous then the effect of differences in the exact location and the spatial resolution for the different methods is very small, and one would expect the comparisons to be good—as is the case for the middle and upper stratosphere. However, in the lower

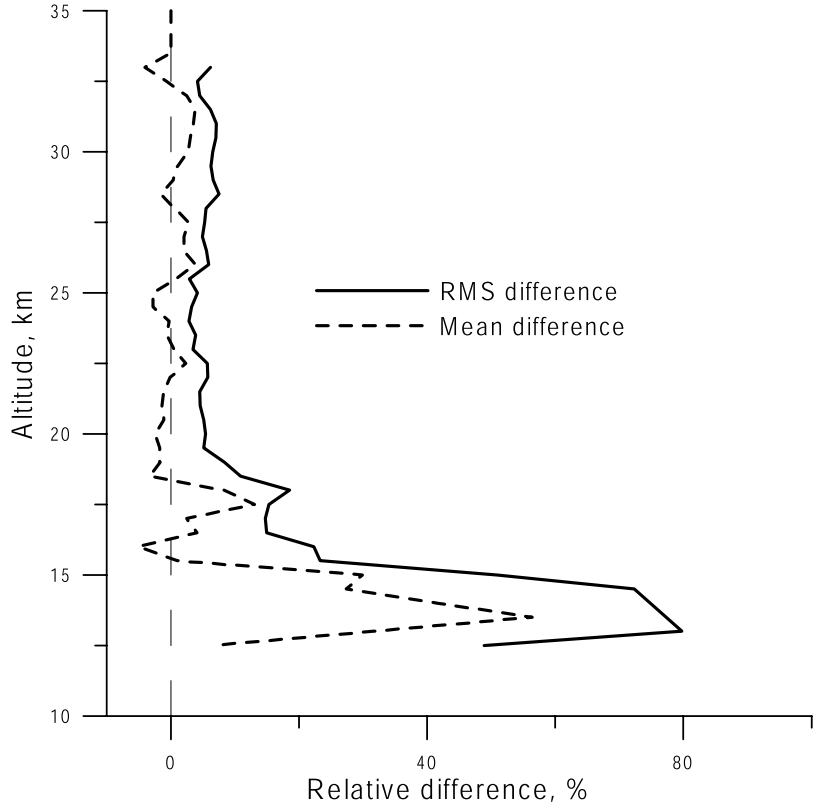

Figure 9. Statistics of the differences between ozonesonde and lidar measurements.

stratosphere the ozone field is highly variable and often horizontally inhomogeneous. This variability leads to different ozone values derived from different measurement methods. This problem causes serious difficulties in validating satellite measurements in the lower stratosphere under conditions of horizontal inhomogeneity of the ozone field. Similar effects would also be expected in the middle stratosphere if ''ozone holes'' are present. For a true validation of the SAGE III ozone measurements in the lower atmosphere, it is necessary to tighten the collocation criteria applied, or schedule specific ground truth missions.

[29] SAGE III ozone profiles retrieved using the SPbSU algorithm have also been compared with HALOE stratospheric ozone profiles for SAGE III local sunset events collocated in time (within 24 hrs.) and space (550 km) with 43 HALOE measurements. HALOE employs solar occultation in the infrared to infer atmospheric gas and aerosol loadings. The results of the comparisons are shown in Figure 10. Mean differences between the two data sets are less than 10% in the wide range of altitudes between 16 and 45 km, with SPbSU retrievals from the SAGE III measurements giving the larger values. The RMS differences between 20 and 45 km are less than 20%. Below 20 km, the differences increase significantly because of the higher ozone variability and the higher aerosol content which leads to a smaller signal-to-noise ratio for ozone.

[30] It is instructive to examine the degree to which the ozone retrievals are influenced by the inversion algorithm. In Figure 11, we present the mean SAGE III stratospheric ozone profiles obtained from the SPbSU and NASA algorithms for the complete set of 157 events available between May and October 2002, the absolute and relative RMS differences between the retrievals and the mean difference between them. Between 15 and 50 km the RMS difference is less than 8% and is only 4–5% between 20 and 40 km. There is a small (about 2%) systematic difference between them throughout most of the stratosphere, with the SPbSU algorithm retrieving slightly lower values. At 10–13 km the RMS difference increases greatly, and, as can be seen in Figure 11 (left), exceeds 100% at low altitudes. Differences between the retrievals may be accounted for by the difference in the ozone absorption coefficients used, and at lower altitudes the differences are likely attributable to the difference in the way that aerosols are accounted for in the two algorithms, because aerosols dominate the extinction at these low altitudes. In the operational algorithm, the atmospheric transmittance function is approximated from the optical depth averaged over the spectral intervals (equations (5) and (6)) as opposed to the SPbSU method in which the integration is performed within each spectral interval (equations (3) and (4)).

4.2. Nitrogen Dioxide

[31] To validate the NO_2 retrievals, we compared our retrievals with those profiles of coincident HALOE local sunset events using the same set of measurements (43 SAGE III and HALOE occultation events) as we used for the ozone validation. As in the case of ozone we restricted our comparisons with HALOE measurements to local sunset only events to limit differences which might arise as a result of differing treatment of diurnal effects in the SAGE III and HALOE algorithms. In Figure 12 we show an example comparison of a single retrieval. Figure 12 shows the NO_2 profile measured by HALOE and one retrieved

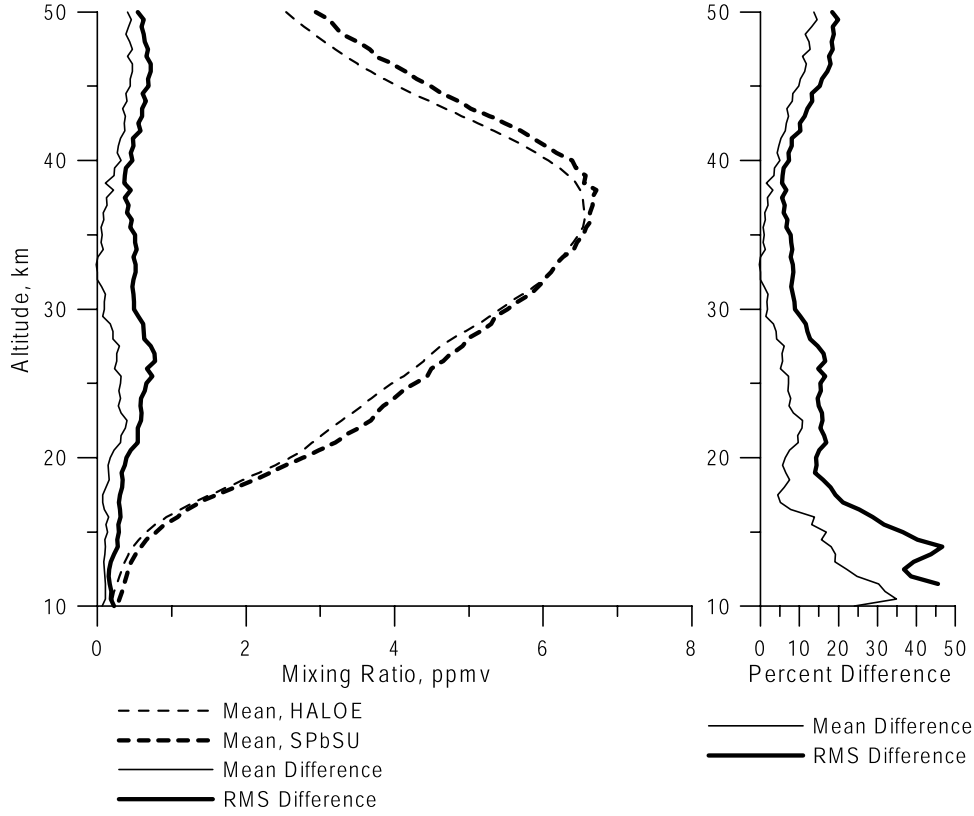

Figure 10. Comparison of SAGE III SPbSU ozone retrievals with HALOE.

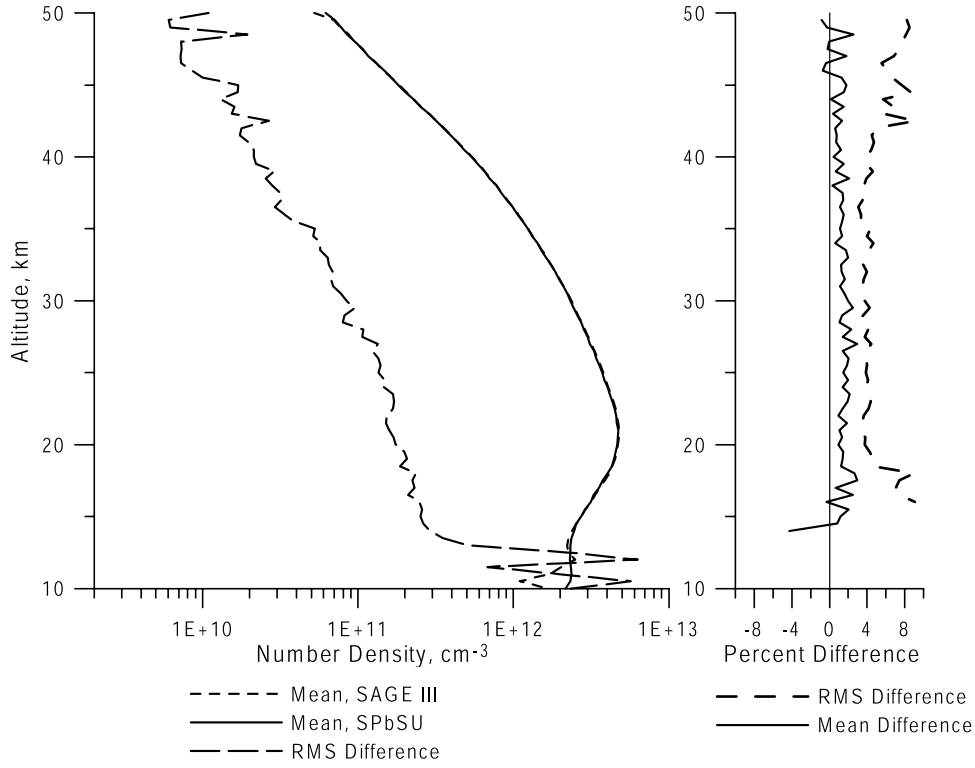

Figure 11. Comparison of SAGE III ozone profiles retrieved from the operational algorithm with those from the SPbSU algorithm.

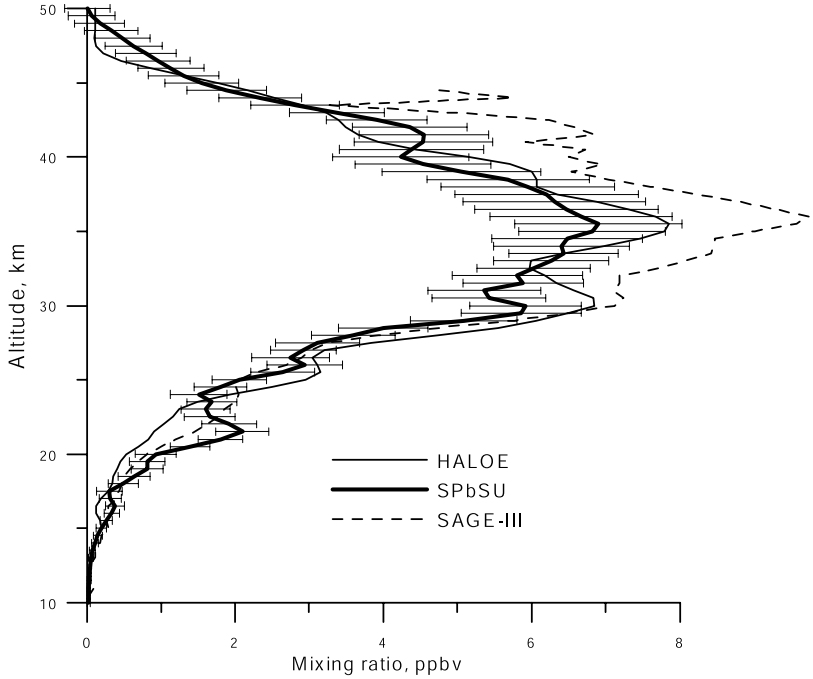

Figure 12. Comparison of the retrieved NO_2 profiles from the SPbSU algorithm, the SAGE III operational algorithm, and HALOE. The SAGE III data corresponds to event 373510, taken on 9 September 2002, at 55°S, 29°W. SAGE III and HALOE measurements were 463 km and 17 min apart.

from the same SAGE III transmission data for the operational SAGE III algorithm and for our (SPbSU) algorithm. The forms of the three retrievals are similar at all altitudes but there are large differences between the magnitudes of the NO_2 mixing ratios at most altitudes. Horizontal line segments in Figure 12 show the estimated errors in our retrieval. (For clarity, estimated errors from SAGE III and HALOE are not shown, but errors from HALOE are similar to those shown, and for SAGE III they are significantly larger.) The differences between the profiles exceed the combined estimated errors at many altitudes. The SPbSU algorithm retrieves lower NO_2 concentrations than HALOE and SAGE III throughout most of the stratosphere. This result holds for the intercomparisons in general, and is evident in Figure 13, where we show the mean differences between HALOE and the SPbSU algorithm for all the coincident local sunset events. In Figure 13, we have compared only local sunset events in order to minimize differences which may be caused by the different (or lack of) treatment of diurnal effects in the algorithms [*Newchurch et al.*, 1996]. Note, however, that these diurnal corrections are unimportant above 25 km and maximize at only 20% at about 20 km. In the statistics of the NO_2 intercomparisons between SPbSU and HALOE shown in Figure 13 it is clear that the shapes of the mean profiles are in good general agreement. In the NO_2 layer between 25 and 40 km the mean difference is mostly less than 20%, peaking at around 40% close to 30 km. The RMS difference between the two is similar but a little larger, 20–35%, and mimics the variance in the HALOE and SPbSU retrievals.

[32] Going back to the single event shown in Figure 12, the SAGE III operational algorithm produces higher concentrations than the SPbSU algorithm. This result appears to be systematic and carries over to the mean of all the profiles we compared (addressed in Figure 14.) In Figure 14, we show a comparison of the SAGE III NO_2 profiles retrieved by the SPbSU and by the operational algorithm for the set of coincident profiles. This comparison suggests a systematic difference in the retrievals, with the operational algorithm producing values consistently higher. Mean differences in NO_2 between SAGE III and SPbSU retrievals are 20–30% throughout the main stratospheric layer (Figure 14 (right)). RMS differences are close to the mean differences and exceed them by less than 5%.

[33] The agreement between the NO_2 profiles obtained from HALOE and from SAGE III shows significant sensitivity to the retrieval algorithm employed. This will be examined in more detail in future investigations that will include the extension of our algorithm to the treatment of diurnal effects and thus allow for a closer comparison of the HALOE and SAGE III data.

5. Summary

[34] A new algorithm has been independently developed for the retrieval of atmospheric gas concentrations and aerosol extinction from the SAGE III transmission data. This new algorithm differs from the NASA operational algorithm in several key aspects—(1) the algorithm takes into account the finite altitude and spectral resolution of measurements by integrating over the width of the viewing window spatially and spectrally; (2) the inverse problem is solved nonlinearly using the optimal estimation algorithm; and (3) the aerosol extinction is parameterized by an optimal expansion using the eigenvectors of the aerosol extinction correlation matrix. This matrix was constructed via numerical simulation for a large database of models of

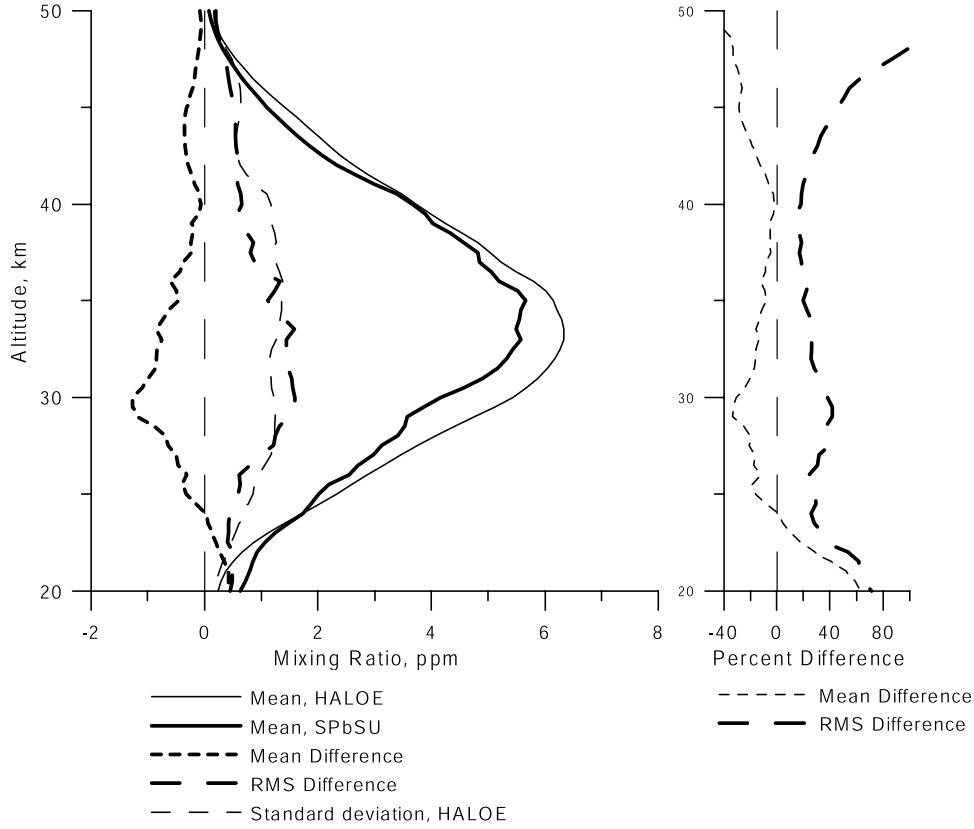

Figure 13. (left) Comparison of SAGE III NO_2 local sunset retrievals using the SPbSU algorithm with NO_2 retrievals from HALOE and (right) mean and RMS difference between the SPbSU SAGE III and HALOE profiles.

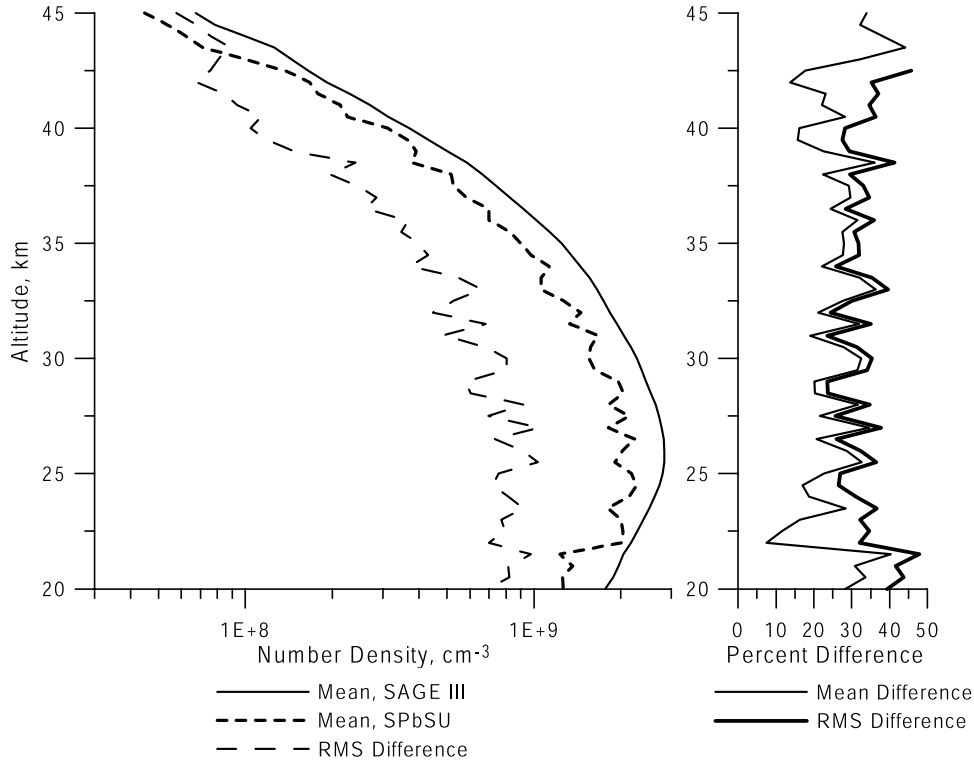

Figure 14. Comparisons of NO_2 profiles retrieved from SAGE III measurements using the SPbSU algorithm with those using the operational algorithm.

stratospheric and tropospheric aerosol [see *Timofeyev et al.*, 2003].

[35] In order to assess the potential accuracy of the retrieval of atmospheric parameters by our algorithm, closed-loop numerical experiments were performed taking into account the SAGE III random measurement noise. These simulations produced errors in retrieving ozone of ~5% on average in the altitude range of 12–70 km, increasing outside this range. The mean errors in retrieving NO_2 concentration were 6–8% at altitudes of 20–45 km. The optimal number of eigenvectors in the expansion of the aerosol extinction coefficient was determined to be 4. Errors in the assignment of tangent height have a strong influence on the errors in retrieving the atmospheric parameters, and can increase the error by two to three times for a height error of 0.5 km.

[36] Extensive comparisons of our retrievals with those from other satellites, ozonesondes, and lidar were made. In addition, the results from our algorithm were compared with those of the SAGE III operational algorithm. Comparison of ozone profiles with ozonesonde measurements (collocated in time (within 24 hours) and space (within 550 km)) demonstrated good agreement (better than 10–20%) in the middle and upper stratosphere. In the lower stratosphere and upper troposphere, the disagreement was greater and could be 40% or more. At altitudes of 25–35 km the RMS differences between the satellite and the ozonesonde measurements were two to three times less than ozone natural variability. However, in the lower stratosphere and upper troposphere, the RMS difference was almost as great as the natural variability.

[37] In most cases, our retrieved ozone data were found to be in good agreement with the lidar measurements (within 5–20% at altitudes of 17–40 km). Below 17 km, the differences increased. Satellite measurements recovered the fine structure in the ozone vertical profiles well. At altitudes of 15–35 km the RMS satellite-lidar differences were 1.5 to 3 times the natural ozone variability. At lower altitudes these values were essentially equal.

[38] Comparisons of retrieved ozone with the HALOE data demonstrated good agreement. On average, differences between individual retrievals did not exceed 10–20%. Typical differences were less than 10%, well within the sum of the estimated errors in both measurements.

[39] Because ozone concentrations from SAGE III showed large differences from ozonesonde and lidar measurements in the lowest part of the stratosphere, it was instructive to investigate how well these independent lidar and ozonesonde measurements agreed with each other. We compared these using the same collocation criteria (within 550 km and 24 hours) and found that mean and RMS differences were 3–6% at 17–32 km. Below 17 km differences increased up to 20–60% for the mean and 80% for the RMS. Thus it appears that large differences in ozone observed below 15–17 km are not necessarily due to the satellite retrieval but exist between other sets of measurements also.

[40] SPbSU retrievals of NO_2 vertical profiles demonstrated spatial-temporal variations that are in good agreement with NO_2 seasonal and latitudinal models. Comparison of SPbSU NO_2 retrievals with HALOE measurements showed good agreement in general, but in a number of cases the differences are considerable. Mean differences between the two satellite measurements were 5–20% and RMS differences, less than 20% above 18 km. In the lower stratosphere, mean and RMS differences increased up to 30% and 45%, respectively. SAGE III NO_2 retrievals using the operational algorithm differ systematically from those using the SPbSU algorithm (see Figure 14) with mean and RMS differences of 20–40%.

Appendix A: Convergence in the Solution of the Optimal Estimation Problem

[41] The solution of the inverse problem through optimal estimation, generalized to nonlinear problems, is that of finding $\hat{x}$ to minimize the function $F(\hat{x})$,

$$F(\hat{x}) = \|\mathbf{B}(\hat{x}) - y\|^2_{S_y^{-1}} + \|\hat{x} - x_a\|^2_{S_a^{-1}}, \tag{A1}$$

where **B** is the forward operator acting on parameters, $\hat{x}$, and y is the set of measurements. To avoid problems in achieving convergence (due to the nonlinearity), we used the minimization of $F_1(x_{k+1})$ [*Polyakov*, 1996],

$$F_1(x_{k+1}) = \|B(x_{k+1}) - y\|^2_{S_y^{-1}} + \|x_{k+1} - x_a\|^2_{S_a^{-1}} + \|x_{k+1} - x_k\|^2_{L^{-1}}. \tag{A2}$$

Here x_k and x_{k+1} are consecutive approximations to the solution. L is any positive determined matrix. The notation, $\|\vec{J}\|_{C^{-1}}$, in equations (A1) and (A2) above denotes the scalar product $(\vec{J}, C^{-1}\vec{J})$. When the iterative process converges, the last term in (A2) is equal to zero and the solution of (A2) coincides with that of (A1).

[42] To choose the matrix L, we used the following algorithm. Matrix L is represented as the product $L = l \cdot L_0$, where l is a positive number and L_0 is the diagonal matrix with the diagonal set equal to the diagonal of the a priori uncertainty matrix, S_a. The number l is chosen at each step of the iteration process so that the condition $F(\hat{x}_{k+1}) \leq F(\hat{x}_k)$ is accomplished. If this condition is not accomplished, l is halved and $\vec{x}_{k+1}$ is calculated afresh. This procedure is repeated until the condition is met. To accelerate this process, the parameter l is doubled if its value does not decrease in the two previous steps. In this manner we achieve the optimal change in the solution at each step corresponding to the nonlinear problem.

[43] **Acknowledgments.** This research was supported by NASA grant NAG 5-11248 and Russian Foundation for Basic Research grant 03-05-64626, "Universities of Russia" UR.01.01.063. SAGE III data level 1B and 2 were obtained from the NASA Langley Research Center Atmospheric Sciences Data Center. The authors are grateful to P. DeCola, W. Chu, and the SAGE III team for the experimental data and useful discussions.

References

Anderson, G. P., S. A. Clough, F. X. Kneizys, J. H. Chetwynd, and E. P. Shettle (1986), AFGL atmospheric constituent profiles (0–120 km), *Environ. Res. Pap.*, *954*, 43 pp., Air Force Geophys. Lab., Hanscom Air Force Base, Mass.

Bass, A. M., and R. J. Paur (1984), The ultraviolet cross sections of ozone, in *The Measurements of Atmospheric Ozone*, edited by C. S. Zerefos and A. D. Ghazi, pp. 606–610, Springer, New York.

Bruhl, C., et al. (1996), Halogen Occultation Experiment ozone channel validation, *J. Geophys. Res.*, *101*, 10,217–10,240.

Burkholder, J. B., and R. K. Talukdar (1994), Temperature dependence of the ozone absorption spectrum over the wavelength range 410 to 760 nm, *Geophys. Res. Lett.*, *21*(4), 581–584.

Keating, G. M., M. C. Pitts, and D. F. Young (1989), Ozone reference models for the middle atmosphere (new CIRA), in *Reference Models of Trace Species for the COSPAR International Reference Atmosphere, Handbook for MAP*, vol. 31, edited by G. M. Keating, pp. 1–36, SCOSTEP Secr., Univ. of Ill., Urbana.

Kostsov, V. S., Y. M. Timofeyev, and R. O. Manuilova (2004), Global distributions of temperature, carbon dioxide, ozone, and non-LTE parameters in mesosphere and lower thermosphere (CRISTA-1 experiment), *Proc. SPIE Int. Soc. Opt. Eng.*, *5235*, 208–219.

Lumpe, J. D., et al. (1997), POAM II retrieval algorithm and error analysis, *J. Geophys. Res.*, *102*, 23,593–23,614.

Newchurch, M. J., et al. (1996), Stratospheric NO and NO_2 abundances from ATMOS solar-occultation measurements, *Geophys. Res. Lett.*, *23*(17), 2373–2376.

Poberovskii, A. V., et al. (1999), Ozone profile determination by occultation sounding from the Mir space station: 1. Instrumentation and data processing method, *Izv. Russ. Acad. Sci. Atmos. Oceanic Phys.*, Engl. Transl., *35*(3), 282–290.

Polyakov, A. V. (1996), To the question of using statistical information, a priori, in solving nonlinear inversed problems of atmospheric optics, *Earth Res. Space*, *3*, 11–15.

Polyakov, A. V., and Y. M. Timofeyev (2003a), Potential accuracies of retrieving the vertical profiles of atmospheric parameters (satellite-based transmittance method): 1. Ozone and nitrogen dioxide contents, *Izv. Russ. Acad. Sci. Atmos. Oceanic Phys.*, Engl. Transl., *39*(2), 227–233.

Polyakov, A. V., and Y. M. Timofeyev (2003b), Potential accuracies of retrieving the vertical profiles of atmospheric parameters (satellite-based transmittance method): 2. Spectral coefficient of aerosol extinction, *Izv. Russ. Acad. Sci. Atmos. Oceanic Phys.*, Engl. Transl., *39*(2), 234–239.

Polyakov, A. V., A. V. Poberovskii, and Y. M. Timofeyev (1999), Ozone profile determination by occultation sounding from the Mir space station: 2. Comparison of the observational results with independent data, *Izv. Russ. Acad. Sci. Atmos. Oceanic Phys.*, Engl. Transl., *35*(3), 322–328.

Polyakov, A. V., Y. M. Timofeev, A. V. Poberovskii, and A. V. Vasil'ev (2001a), Retrieval of stratospheric vertical profiles of aerosol extinction coefficient from the Ozon-Mir measurements (Mir space station), *Izv. Russ. Acad. Sci. Atmos. Oceanic Phys.*, Engl. Transl., *37*(2), 213–222.

Polyakov, A. V., A. V. Vasil'ev, and Y. M. Timofeev (2001b), Parameterization of the spectral dependence of the aerosol attenuation coefficient in problems of atmospheric occultation sounding from space, *Izv. Russ. Acad. Sci. Atmos. Oceanic Phys.*, Engl. Transl., *37*(5), 599–609.

Rodgers, C. D. (2000), *Inverse Methods for Atmospheric Sounding: Theory and Practice*, *Ser. Atmos. Oceanic Planet. Phys.*, vol. 2, 238 pp., World Sci. Press, Hackensack, N. J.

SAGE III ATBD Team (2002a), SAGE III algorithm theoretical basis document (ATBD) transmission level 1B products, version 2.1, *LaRC 475-00-108*, NASA Langley Res. Cent., Hampton, Va., 26 March. (Available at www-sage3.larc.nasa.gov/library)

SAGE III ATBD Team (2002b), SAGE III algorithm theoretical basis document (ATBD) solar and lunar algorithm, version 2.1, *LaRC Rep. 4750-00-109*, NASA Langley Res. Cent., Hampton, Va., 26 March. (Available at www-sage3.larc.nasa.gov)

Schneider, W., G. K. Moortgat, G. S. Tyndall, and J. P. Burrows (1987), Absorption cross-section of NO_2 in the UV and visible region (200–700 nm) at 298 K, *J. Photochem. Photobiol. A0*, *40*, 195–217.

Timofeyev, Y. M., A. V. Polyakov, H. M. Steele, and M. J. Newchurch (2003), Optimal eigenanalysis for the treatment of aerosols in the retrieval of atmospheric composition from transmission measurements, *Appl. Optics*, *42*(15), 2635–2646.

Virolainen, Y. A., A. V. Polyakov, and Y. M. Timofeyev (2004), Statistical models of tropospheric aerosol, *Izv. Russ. Acad. Sci. Atmos. Oceanic Phys.*, Engl. Transl., *40*(2), 216–227.

D. V. Ionov, A. V. Polyakov, Y. M. Timofeyev, and Y. A. Virolainen, Department of Atmospheric Physics, St. Petersburg State University, 1 Ulyanovskaya, St. Petersburg 1985504, Russia.

M. J. Newchurch, National Space Science and Technology Center, Atmospheric Science Department, University of Alabama in Huntsville, 320 Sparkman Dr., Huntsville, AL 35805, USA.

H. M. Steele, Department of Geography, California State University, Northridge, CA 91330-8249, USA. (helen.m.cox@csun.edu)